J Bioenerg Biomembr (2011) 43:203–215
DOI 10.1007/s10863-011-9347-6

Involvement of thermoplasmaquinone-7 in transplasma membrane electron transport of *Entamoeba histolytica* trophozoites: a key molecule for future rational chemotherapeutic drug designing

Nilay Nandi · Tanmoy Bera · Sudeep Kumar · Bidyut Purkait · Ashish Kumar · Pradeep Das

Received: 7 January 2011 / Accepted: 25 January 2011 / Published online: 27 April 2011

Abstract The quinone composition of the transplasma membrane electron transport chain of parasitic protozoa *Entamoeba histolytica* was investigated. Purification of quinone from the plasma membrane of *E. histolytica* and its subsequent structural elucidation revealed the structure of the quinone as a methylmenaquinone-7 (thermoplasmaquinone-7), a napthoquinone. Membrane bound thermoplasmaquinone-7 can be destroyed by UV irradiation with a concomitant loss of plasma membrane electron transport activity. The abilities of different quinones to restore transplasma membrane electron transport activity in UV irradiated trophozoites were compared. The lost activity was recovered completely by the addition of thermoplasmaquinone-7, but ubiquinones are unable to restore the same. These findings clearly indicate that thermoplasmaquinone-7 acts as a lipid shuttle in the plasma membrane of the parasite to mediate electron transfer between cytosolic reductant and non permeable electron acceptors. This thermoplasmaquinone-7 differs from that of the mammalian host and can provide a novel target for future rational chemotherapeutic drug designing.

Keywords *Entamoeba histolytica* · Transplasma membrane electron transport · UV irradiation · Thermoplasmaquinone-7

N. Nandi · S. Kumar · B. Purkait · A. Kumar · P. Das (✉)
Department of Molecular Biology,
Rajendra Memorial Research Institute of Medical Sciences,
Agam Kuan,
Patna 800 007 Bihar, India
e-mail: drpradeep.das@gmail.com

T. Bera
Division of Medicinal Biochemistry,
Department of Pharmaceutical Technology, Jadavpur University,
Kolkata 700 032 West Bengal, India

Introduction

Entamoeba histolytica, the causative agent of human amoebiasis, is the fourth leading cause of death due to a protozoan infection after malaria, Chagas disease, and leishmaniasis and the third cause of morbidity after malaria and trichomoniasis. The disease is responsible for approximately 70 thousand deaths annually (World Health Organization, The world health report 1998). The parasite representing the early branches of eucaryotic evolution is amitochondriate, microaerophilic protist and uses fermentation enzymes to survive anaerobic conditions within the intestinal lumen where they persist for months or even years as an asymptomatic luminal gut infection. However, occasionally, *E. histolytica* trophozoites destroy human tissues by penetrating the mucosa and submucosa of the large intestine and disseminate to other organs, most commonly to the liver where they induce abscess formation (Ravdin 1988). *E. histolytica* does not usually tolerate elevated oxygen concentration. However, during tissue invasion, trophozoites are challenged by a high O_2 environment (Ramos-Martínez et al. 2009) and by the Reactive Oxygen Species (ROS) produced by endogenous enzymes and activated phagocytes during the respiratory burst (Santi-Rocca et al. 2009). Therefore, in order to successfully establish an infection, trophozoites must survive despite the local production of ROS in liver and other organs. Molecules involved in resistance to ROS in *E. histolytica* have been well characterized and mainly involve stress regulatory enzymes like Fe SOD (Bruchhaus and Tannich 1994), NADPH:flavin oxidoreductase (Bruchhaus et al. 1998), and peroxiredoxin (eh29) (Bruchhaus et al. 1997). The increased resistance to $^{\cdot}OH$ might be due to scavenging of this free radical by antioxidant compounds.

Electron transport across the plasma membrane has been described in many eukaryotic cells (Crane et al. 1989), such as erythrocytes, liver, heart, transformed liver cells, HeLa cells, neutrophils, yeast and plant cells. This transplasma membrane electron transport (TPMET) plays a crucial role in iron transport into the cell (Leuisse and Labbe 1992), stimulation cell growth (Larm et al. 1994) and reduction of extracellular antioxidant compounds (Crane and Navas 1997; Stocker and Suarna 1993; Roy et al. 1997) to maintain the optimal redox environment. We have demonstrated earlier the existence of TPMET in *E. histolytica* and found that it is critical in maintaining an optimal extracellular redox state with the consequent protection of the parasite against high oxygen concentration in liver and tissues (Bera et al. 2006). In TPMET quinone serves as a lipid soluble shuttle to transfer electrons across the plasma membrane and plays the extremely basic function in mediation and preservation of antioxidant function in cells (Crane and Navas 1997). Isoprenoid quinones residing in the cytoplasmic membrane play important roles in the electron transport system in bacterial (Collins and Jones 1981) and mammalian cells (Sun et al. 1992). Bacterial quinones generally comprise two major groups, mainly ubiquinone, which is 2,3-dimethoxy-5-methyl-6-multiprenyl-1,4-benzoquinones, and menaquinones, which are 2-methyl-3-multiprenyl-1,4-napthoquinones, 2-demethyl-3-multiprenyl-1,4-naphthoquinones and 2,8-dimethyl-3-multiprenyl-1,4-naphthoquinone (Collins and Fernandez 1984; Itoh et al. 1985). Menaquinones (vitamin K_2) form a large class of molecules in which the length of the C-3 isoprenyl side-chain varies from 1 to 15 isoprene units (Collins and Jones 1981). In addition to differences in the number of isoprene units, varying degrees of saturation of the side-chain are found (Collins and Jones 1981). Other modifications of menaquinones include the replacement of the methyl group at C-2 with an -H atom (as in demethylmenaquinones) or -SCH_3 group (as in methionaquinone) (Ishii et al. 1987). Collins (1985a) reported the isolation of a new quinone, designated as thermoplasmaquinone, from the thermophilic, acidophilic archaebacterium *Thermoplasma acidophilum*. Chlorobiumquinone, an isomer of thermoplasmaquinone had also been reported in anaerobic photosynthetic green sulphur bacteria *Chlorobium thiosulphatophilum* and *Chloropseudomonas ethylicum* along with menaquinone (Powls and Redfearn 1969). Evidence to support the existence of a transplasma membrane redox system in *E. histolytica* arises from the reduction of three impermeable electron acceptors such as ALA, NQSA and ferricyanide by whole cells. Inhibitor studies suggest that quinones of the plasma membrane are involved in the reduction of these non-permeable electron acceptors at the exoplasmic face of this organism (Bera et al. 2006). Irradiation with near-ultraviolet light impairs the TPMET of *E. histolytica* and suggests probable involvement of napthoquinone like compounds (Bera et al. 2006) for maximal performance, because CoQ was not inactivated by UV irradiation (Brodie 1963).

In the present study, we have purified and elucidated the structure of the quinone involved in TPMET of *Entamoeba*. Examination of the lipid extracts from the purified plasma membrane of this organism revealed the structure of the quinone as a methylmenaquinone-7, a napthoquinone. Further investigation indicates that the purified methylmenaquinone-7 restores the TPMET activity completely for the UV irradiated trophozoites, whereas the menaquinone-4 restores the same partially and CoQ_{10} was unable to restore it. This suggests that methylmenaquinone-7 might function as the main plasma membrane electron transport quinone in *E. histolytica* trophozoites. This information may help in exploring future rational chemotherapeutic targets for drug designing.

Experimental procedures

All biochemicals unless otherwise mentioned were from Sigma Chemicals (St. Louis, MO, USA).

Parasite

Axenically grown pathogenic trophozoites of *E. histolytica* (strain HM1: IMSS) was maintained in TYI-S-33 medium containing sterilized 10% heat inactivated bovine serum and vitamin mixture (Diamond et al. 1978). They were subcultured after every 48 h. Cells were harvested by centrifugation at 400×g, washed thrice in HEPES-EDTA buffer at 400×g and the harvested cells were immediately used for assay. Viability of harvested cells was monitored by Trypan Blue exclusion method (Strober 2001).

Protein estimation

The amount of protein was determined by the Biuret method (Fine 1935) using BSA as a standard.

Isolation of plasma membrane

Plasma membrane was isolated following the method of Aley et al. (1980). The cell pellet was resuspended to 2×10^7 cells/ml in PD Buffer (19 mM potassium phosphate buffer, pH 7.2, which contained 0.27 M NaCl) that contained 10 mM $MgCl_2$ and rapidly mixed with an equal volume of 1 mg/ml concanavalin A in the same buffer. Cell aggregation was apparent within 1 min. After 5 min, cells were gently spun at 50×g for 1 min to remove excess concanavalin A. The supernatant was discarded, and the cell pellet resuspended in 12 ml of 10 mM Tris–HCl buffer,

pH 7.5, that contained 2 mM phenylmethyl sulfonyl fluoride (PMSF) in Tris buffer and $MgCl_2$ added to 1 mM. After swelling for 10 min in the hypotonic buffer [Tris.Cl, pH 7.4 (10 mM), $MgCl_2$ (30 mM), PMSF (0.005%)], cells were homogenized by 18–20 strokes of a glass Dounce homogenizer with a tight-fitting pestle. Cell lysis and the formation of membrane sheets was verified by phase-contrast microscopy The homogenate was layered over a two-step gradient consisting of 8 ml of 0.5 M mannitol over 4 ml of 0.58 M sucrose, both in Tris buffer, and spun at 250×g for 30 min. For analysis, material remaining at the top of the 0.5 M mannitol (supernatant I) was centrifuged at 40,000×g for 1 h to separate soluble molecules from small membrane fragments and vesicles (supernatant II and pellet II). Large plasma membrane fragments and other heavy debris formed a tight pellet at the bottom of the gradient (pellet I). This pellet was resuspended in 1 ml Tris buffer that contained 1 M α-methyl mannoside and left on ice for 40 min with occasional mixing. The plasma membranes, now free of the bulk of the concanavalin A, were diluted into three volumes of Tris buffer and homogenized by 80 strokes with a glass Dounce homogenizer. This second homogenate was layered on a single-step gradient that consisted of 20% sucrose in Tris buffer and spun for 30 min at 250×g. Vesiculated plasma membranes floating above the initial sucrose layer (supernatant III) were collected and concentrated by centrifugation at 40,000×g for 1 h. The pellet (pellet IV), containing the enriched plasma membranes, was resuspended directly in Storage buffer, pH 7.8 [NaCl (0.15 M), Tris.Cl (20 mM)]. All samples were either assayed immediately or frozen at −20 °C for future use.

Marker enzyme assay

Alcohol dehydrogenase activity

Alcohol dehydrogenase activity of *E. histolytica* was assayed as described by Reeves et al. (1971) to analyze the purity of the isolated plasma membrane. 100 mM Tris HCl Buffer, pH 7.8 at 40 °C (2.4 ml), 15 mM β-Nicotinamide Adenine Dinucleotide Phosphate Solution (β–$NADP^+$) (0.1 ml) and 1.5 M 2-Propanol (0.3 ml) was mixed by inversion and equilibrated to 40 °C. Whole cell homogenate or membrane fractions were then added immediately to the mixture, mixed by inversion and the increase in absorbance at 340 nm was monitored for approximately 5 min. An appropriate blank was also prepared in which the plasma membrane fraction is not added. The ΔA_{340nm}/minute was obtained using the maximum linear rate for both the Test and Blank. One unit of enzyme will oxidize 1.0 μmole of 2-propanol to acetone per minute at pH 7.8 at 40 °C in the presence of β-$NADP^+$.

Ca^{2+}-dependent (Mg^{2+}-inhibited) ATPase activity

ATPase activity was measured by determining the release of inorganic phosphate from ATP using a slightly modified version of the procedure of Evans (1969). The assay mixture contained (in 1 ml): Tris.Cl buffer (pH 8.5), 100 mM; ATP, 4 mM; $CaCl_2$, 4 mM; whole cell homogenate or membrane fractions. After 15 min at 37°C, the reaction was stopped by adding 1 ml of chilled 10% (w/v) trichloroacetic acid and the tubes were left in ice for 15 min. Samples were centrifuged at 3000×g for 5 min and inorganic phosphate was determined in the supernatant according to Tausky and Shor (1953). Protein was estimated by the method of Lowry et al. (1951). Enzyme activities are expressed as pmol inorganic phosphate (P_i) liberated per mg protein in 15 min under the standard assay conditions.

Acid phosphatase activity

Acid Phosphatase activity was measured following methods of Bull et al. (2002) for the whole cell homogenate and membrane fractions. Acid phosphatases (APs) are members of the hydrolase class of enzymes and catalyze the hydrolysis of orthophosphate monoesters under acidic conditions. The assay utilizes para-nitrophenyl phosphate (pNPP) as a chromogenic substrate for the enzyme. In the first step, AP dephosphorylates pNPP. In the second step, the phenolic OH-group is deprotonated under alkaline conditions resulting in p-nitrophenolate that yields an intense yellow color which can be measured at 405–414 nm.

N-Acetyl-β-glucosaminidase activity

N-Acetyl-β-glucosaminidase was assayed using 4-methyl-umbelliferyl-2-acetamido-2-deoxy-β-D-glucopyranoside as substrate (Peters et al. 1972). Whole cell homogenate or membrane fractions are resuspended in citrate buffer containing 0.26 mmol of 4-methyl-umbelliferyl-2-acetamido-2-deoxy-β-D-glucopyranoside as substrate and incubated for 10 min at 37°C. The reaction was stopped by adding 1.5 ml of glycine buffer (0.5 mol/L, pH 10.4). For each test sample a blank was measured in which the plasma membrane is added after instead of before the glycine buffer. Fluorescence was measured at 360 nm excitation and 455 nm emission using LS 55 spectrofluorimeter. Enzyme activity units (U) were calculated in terms of the number of micromoles of 4-methylumbelliferone hydrolyzed per minute

at 37°C. Protein was estimated by the method of Lowry et al. (1951).

Extraction of quinone from the plasma membrane

Quinone was isolated from the plasma membrane of *E. histolytica* following the method of Biswas et al. (2008). Briefly, 500 mg lyophilized plasma membrane was extracted 8 times at 0 °C with 25 ml n-hexane dried over sodium. The particles were suspended in n-hexane by homogenization with a Teflon piston fitting extraction tube. The n-hexane was removed from the residue by centrifugation (10,000×g for 10 min) followed by evaporation in a rotary vacuum evaporator attached to $CaCl_2$ tube. The n-Hexane concentrate was dissolved in 0.5 ml ethanol. 5 ml of 5% $K_3Fe(CN)_6$ solution was added to ethanol solution and the mixture allowed to stand for 10 min at room temperature. The mixture was re-extracted with the addition of ethanol and n-hexane as described above. Extracted quinone was dissolved in 0.5 ml chloroform:methanol [2:1 (v/v)] for further analysis.

Reverse Phase HPLC for purification of Quinone

Extracted quinones were analyzed using HPLC (Hitachi make) equipped with a UV–VIS detector following a modified method of Collins (1985b). Briefly, samples (20 μl) were separated on a Nucleosil 5 μm, 120 A^0 C18 column (inside diameter, 250 by 4.6 mm, including a 30 mm C-18 guard column). A gradient mobile phase at a constant flow rate of 0.5 ml/min was utilized. The initial mobile phase composition was 100% methanol and was changed in a linear fashion over time to methanol: isopropanol (60:40) at 30 min and it was held for a further 30 min, after which the mobile phase was returned in a linear fashion to 100% methanol over a 15 min interval to prepare the column for the next sample. Detection was monitored at 270 nm and 275 nm which are λmax for menaquinone and ubiquinone respectively. Purified peaks were collected for further mass spectrometric and NMR studies. Separation of mixture of quinone standards, menaquinone-4 (Vit. K_2) and CoQ_{10}, were also performed using similar chromatographic conditions.

Mass spectroscopy of the purified quinone

Mass spectra of the HPLC purified quinone was recorded on an AEI MS9 instrument using a direct insertion probe, an ionizing voltage of 70 eV, and a temperature of 180 °C. The analysis was run under computer control with an automatic data acquisition system. The molecular ions generated are separated according to their mass (m) -to-charge (z) ratios (m/z). The separated ions are detected and this signal sent to a data system where the m/z ratios are stored together with their relative abundance for presentation in the format of a m/z spectrum.

^{1}H-NMR spectroscopy

^{1}H-NMR spectra of lyophilized samples in $CDCl_3$ were recorded on a DRX500 NMR spectrometer using tetramethylsilane as an internal standard.

Spectral fingerprint of the purified quinone by UV absorption spectrophotometry

To analyze the spectral fingerprint of the HPLC purified quinone, it was evaporated to dryness and resuspended in isooctane. A wavelength scan was performed between 220 and 360 nm to determine the spectral fingerprint of the purified quinone.

UV irradiation of *E. histolytica*

E. histolytica trophozoites were UV irradiated by modifying the procedure of Brodie and Ballantine (1960). Briefly, *E. histolytica* trophozoites in a buffer containing 120 mM NaCl, 20 mM potassium acetate, 5 mM $MgCl_2$, 5 mM D-glucose, 20 mM HEPES, pH 6.4 and at a protein concentration of 10 mg/ml were placed in a petri dish at 4 °C. A 60 cm long Philips lamp (15 W; maximum emission 360 nm) was placed at a distance of 3 cm from the petridish and the petridish containing cells were UV irradiated for 30 min. Control cells were treated similarly without UV irradiation.

MTT assay

Viability of UV untreated and treated *E. histolytica* cells (2×10^6 each set) were determined using the *in vitro* toxicology assay kit MTT-based (Sigma, USA). MTT is an organic compound, which is converted to the blue colored formazan salt derivative only by the active cellular dehydrogenase of living cells and was measured spectrophotometrically at 570 nm. The cells from each set were incubated with and assayed following the kit protocol. In each test there were three replicates and data are expressed as mean of three observation ±S.D.

Measurement of ferricyanide reduction by *E. histolytica* cells

Ferrocyanide quantitation was performed using 1,10-phenanthroline complex as described by Avron and Shavit (1963). The incubation mixture contained 120 mM NaCl, 20 mM HEPES, 20 mM potassium acetate, 5 mM $MgCl_2$,

pH 6.4, 3 mM $K_3Fe(CN)_6$, 5 mM D-glucose and 3 mg *E. histolytica* cells in a final volume of 1.5 ml. The reaction mixture was incubated for 10 min at 37 °C followed by incubation in ice and centrifugation at 2000×g for 10 min. Ferrocyanide in the supernatant was measured by 1.5 ml of 1,10-phenanthroline reagent, which contained 1.5 mmoles sodium acetate, 97 μmoles citric acid, 0.75 μmoles ferric chloride and 12.6 μmoles 1,10-phenanthroline. The absorbance was recorded at 510 nm. The blanks were carried out with all reagents except *E. histolytica* cells.

Measurement of oxygen uptake

Oxygen uptake by *E. histolytica* trophozoites was determined in a Warburg constant volume manometer with air as gas phase at 37°C, with 0.2 ml 20% KOH in the centre well and shaking at 80 cycles/min (Umbreit et al. 1957). For respiration studies, the cells were washed thrice in HEPES-EDTA buffer, pH 7.2 [NaCl (120 mM), KCl (5 mM), $EDTANa_2$ (1 mM), HEPES (20 mM), Glucose (5 mM)]. The Warburg flask contained 15 mg trophozoite protein in a total volume of 3 ml HEPES-EDTA buffer; pH 7.2. Water insoluble compounds were given as a solution in dimethylformamide (5 μl/ml buffer). Appropriate controls were used for each experiment that includes controls devoid of trophozoite protein and dimethylformamide as a vehicle control.

Results

Isolated plasma membrane

When amoebae were homogenized under hypotonic conditions, the plasma membrane because fragmented, and a distinct plasma membrane fraction could not be separated by techniques of differential or isopycnic centrifugation. To overcome this problem, the plasma membrane was stabilized by cross-linking the surface glycoconjugates of intact cells with concanavalin A. *Entamoeba* treated with concanavalin A were homogenized and spun gently through the mannitol/sucrose gradient. Large membrane scrolls were concentrated in the pellet fraction, whereas smaller membrane vesicles were retained above the mannitol phase of the gradient. In accordance with Aley et al. (1980) it was found that pellet I consisted of crude plasma membrane, whereas the membrane components of supernatant I and pellet II consisted largely of internal vesicles. The crude plasma membrane fraction was treated with α-methyl mannoside to release bound concanavalin A and vesiculated in a second homogenization step. This homogenate was gently spun onto a 20% sucrose cushion. The pellet (pellet III) consisted of non-vesiculated plasma membrane and aggregated material. The plasma membranes retained above the sucrose (supernatant III) will consist of smaller fragments and vesicles. This fraction was concentrated by centrifugation at 40,000 g for 1 h (pellet IV). This pellet IV is the isolated plasma membrane.

Distribution of marker enzymes

Protein recovery and four enzymatic activities were monitored throughout the plasma membrane-fractionation procedure. Alcohol dehydrogenase, a soluble enzyme (Reeves et al. 1971), was found solely in supernatant II (data not shown). Insignificant activity was found in all the membrane-containing fractions (data not shown). In mammalian cells and cell lines, acid phosphatase is a soluble enzyme sequestered within lysosomes. In *E. histolytica*, however, this activity was strongly membrane associated. Greater than ~85% of the activity was pelleted by centrifugation of frozen and thawed cells at 40,000 g for 1 h. When cell fractions were assayed for acid phosphatase, ~70% of the activity was found associated with the internal membrane vesicles (data not shown). The final plasma membrane fraction contained only ~5% of the total activity yielding a three fold enrichment (data not shown). The pH optimum and the substrate specificity of the acid phosphatase activities of the internal vesicles and of the purified plasma membrane were compared. The activity from both fractions had an optimal pH of 5.0 and used either p-nitrophenyl phosphate or β-glycerol phosphate as substrate equally well. The subcellular fractions for a second lysosomal hydrolase, N-acetyl-β-glucosaminidase (NAGase), had also been assayed which is a soluble intralysosomal enzyme both in mammalian cells and in *E. histolytica* (Brzóska et al. 2003). NAGase levels, corrected for latency, indicated that the final plasma membrane fraction was contaminated with ~7% of total lysosomes (data not shown). A Calcium-dependent ATPase recently described by McLaughlin and Muller (1979) was included in this analysis as it is one of the few known membrane associated enzymatic activities in *E. histolytica* that does not have an acid pH optimum. The internal membrane fraction (pellet II) contains ~60% of the total ATPase activity, comparable to the percentage for acid phosphatase (data not shown). However, >19% of the activity was localized in the plasma membrane fraction, with an enrichment of ~20-fold (data not shown). This is three times the enrichment of acid phosphatase, and therefore it had been suggested that a major portion of the ATPase activity is associated with the plasma membrane.

Purification of quinone by HPLC

The mixture of quinone standards Menaquinone-4 (naphthoquinone) and CoQ_{10} (ubiquinone) after separation in the reverse phase HPLC showed peaks at retention time

16.06 min and 42.28 min respectively (Fig. 1, Panel A). The quinone isolated from the plasma membrane of the *E. histolytica* trophozoites gives a peak at retention time 17.47 min which is close to the retention time of the menaquinone class of compounds (Fig. 1, Panel B). The slight increase in the retention time compared to Menaquinone-4 probably reflects towards a higher isoprenoid chain length of the purified quinone.

Mass spectroscopy of the purified quinone

The mass spectrum of the purified quinone had a base peak at *m/z* 239 with a second intense peak at *m/z* 201 (Fig. 2, Panel A & B). The most intense peak in the high mass region occurred at *m/z* 662, and was attributable to molecular ions (M^+) (Fig. 2, Panel A & B). Peaks of low intensity at *m/z* 593, 525, 459, 389, 321 and 253 were due to the sequential loss of 1 terminal (69 mass units) and 5 internal (68 mass units) isoprene units respectively (Fig. 2, Panel A & B). A peak of lower intensity at 647 was also observed corresponding to the loss of CH_3 from M^+ (Fig. 2, Panel A).

NMR spectra of the purified quinone

The ^{1}H-NMR spectrum of the quinone has been demonstrated in Fig. 3. Complex absorption was observed in the δ 7.2–8.1 region (Fig. 3, Table 1), due to the presence of 3 aromatic protons, the splitting pattern of which indicated the presence of a methyl group in a peri-position on the ring system (C-5 or C-8). The methyl group causes a shielding of the 3 aromatic protons with the ortho proton (H_3) the most shielded. The doublet at δ 8.0 corresponds to a peri proton (i.e., H_1 in position C-5 and/or C-8), whereas the doublet at δ 7.26 and the triplet at δ 7.68 correspond to aromatic protons at C-6 and C-7 (not necessarily respectively) (Fig. 3, Table 1). The aromatic methyl group in the peri-position (C-5 or C-8) produced a strong singlet at δ 2.73 (Fig. 3, Table 1). The remaining signals in the spectrum of thermoplasmaquinone-7 are essentially similar to those of menaquinones, and correspond to the C-2 ring methyl group (δ 2.18, singlet) and contributions from the C-3 multiprenyl side-chain (i.e. δ 4.9–5.1, olefinic protons; δ 3.36, -CH_2- adjacent to ring; δ 1.92–2.05, -CH_2-allylic; δ 1.79, trans-CH_3 next to ring; δ 1.67, cis-CH_3 end of chain; δ 1.56–1.59, trans internal CH_3) (Fig. 3, Table 1).

Activity analysis of the purified quinone by its spectral fingerprint

The quinone after extraction from the plasma membrane of the trophozoites and subsequent purification by HPLC was subjected to wavelength scan between 220 and 360 nm to

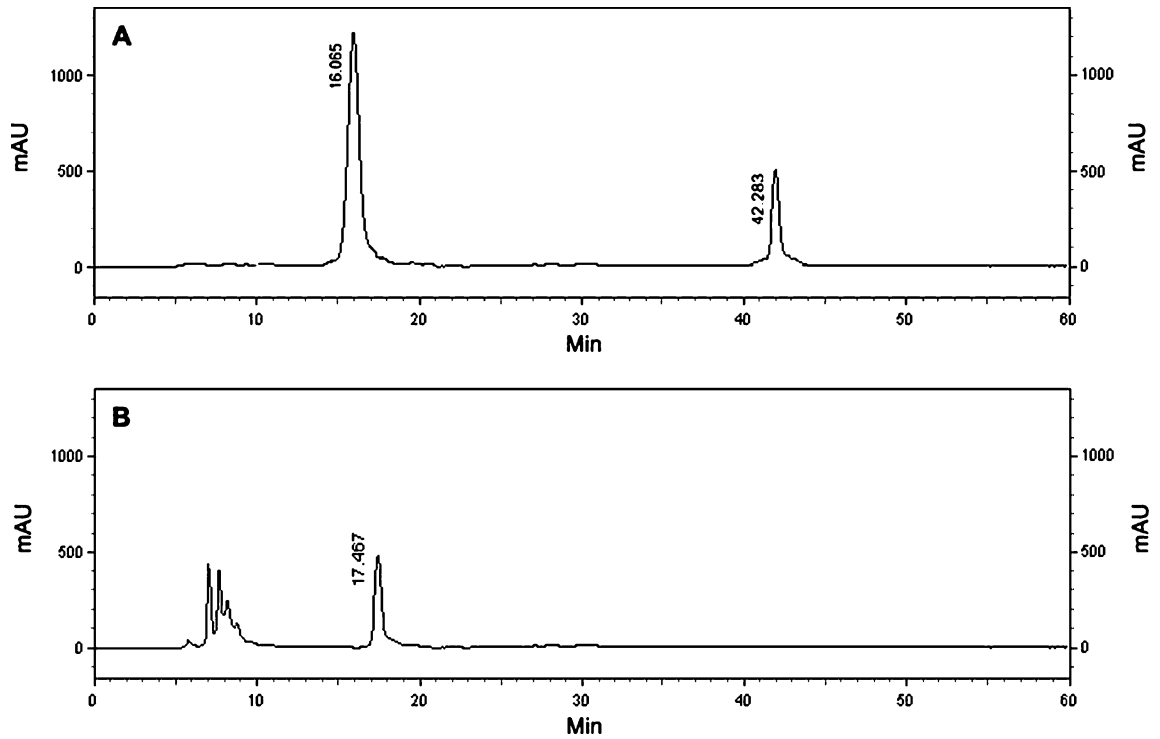

Fig. 1 Purification of quinone using a polar mobile phase and a non-polar octadecylsilyl stationary phase using reverse phase HPLC technique. Panel A represents separation of a mixture of quinone standards, i.e. maenaquinone-4 (naphthoquinone) and CoQ_{10} (ubiquinone). Panel B represents purification of quinone from the lipid fraction isolated from the plasma membrane of the *E. histolytica* trophozoites

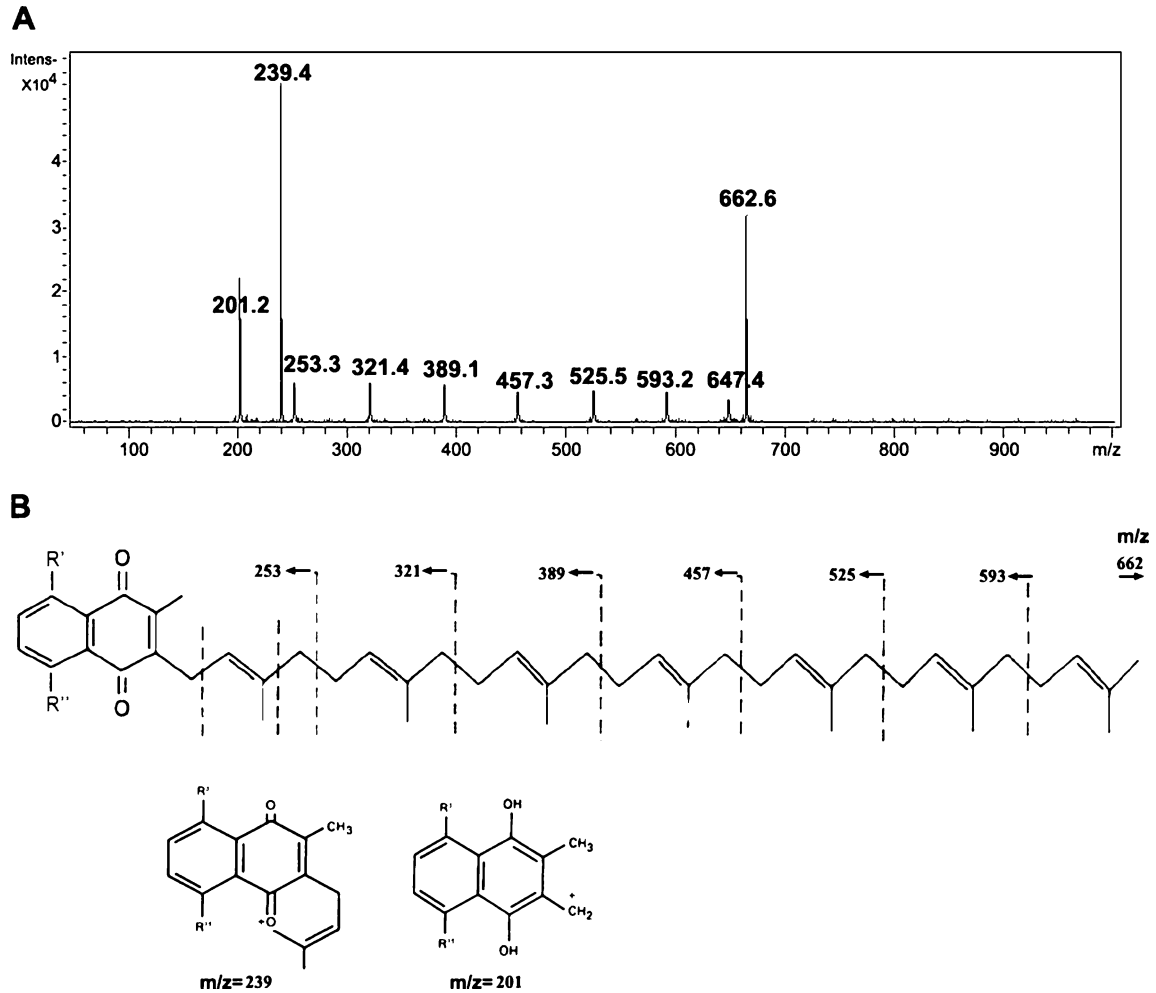

Fig. 2 Mass spectral analysis of the purified quinone using an electron impact ionization source. Panel A represents the molecular ion and the fragment ion peaks in the mass spectra, whereas Panel B gives the structural representation of the probable molecular and fragment ions

demonstrate its spectral fingerprint. The ultraviolet spectra exhibit five absorption maxima at 242, 248, 259, 269, and 338 nm and one point of inflection at 238 nm (Fig. 4). Absorption bands at 242, 248, and 238 nm (shoulder) are due to benzenoid contributions, whereas bands at 259 and 269 nm are due to quinone absorption (Dunphy and Brodie 1971).

Restoration of TPMET of UV irradiated *E. histolytica* trophozoites

The viability of the *E. histolytica* trophozoites was found to be ~95% for both UV treated and untreated trophozoites. However, the transplasma membrane electron transport activities for reactions such as ferricyanide reduction and O_2 uptake were rapidly lost when the *E. histolytica* trophozoites were irradiated with near-UV light (Table 2). The lost activity was recovered completely by the addition of thermoplasmaquinone-7 (Table 2). Incorporation of menaquinone-4 restored transplasma membrane ferricyanide reduction and O_2 uptake partially; but CoQ_{10}, a Ubiquinone, was unable to restore the lost activity (Table 2). These results from reconstitution experiments also confirm that a napthoquinone is involved in TPMET of *E. histolytica* and thermoplasmaquinone-7 might function as the main plasma membrane electron transport quinone in the trophozoites.

Discussion

We have demonstrated earlier that in *E. histolytica* the electron generated by oxidation of NADH or NADPH inside the cell travels to the extracellular milieu by a TPMET chain in which a napthoquinone serves as a lipid soluble shuttle to transfer electrons across the plasma membrane and it helps in maintaining the optimal extracellular redox environment, which in turn is critical for the invasion and survival of the parasite during establishment of amoebic liver abscess (Bera et al. 2006). However, the mitochondrial and transplasma membrane

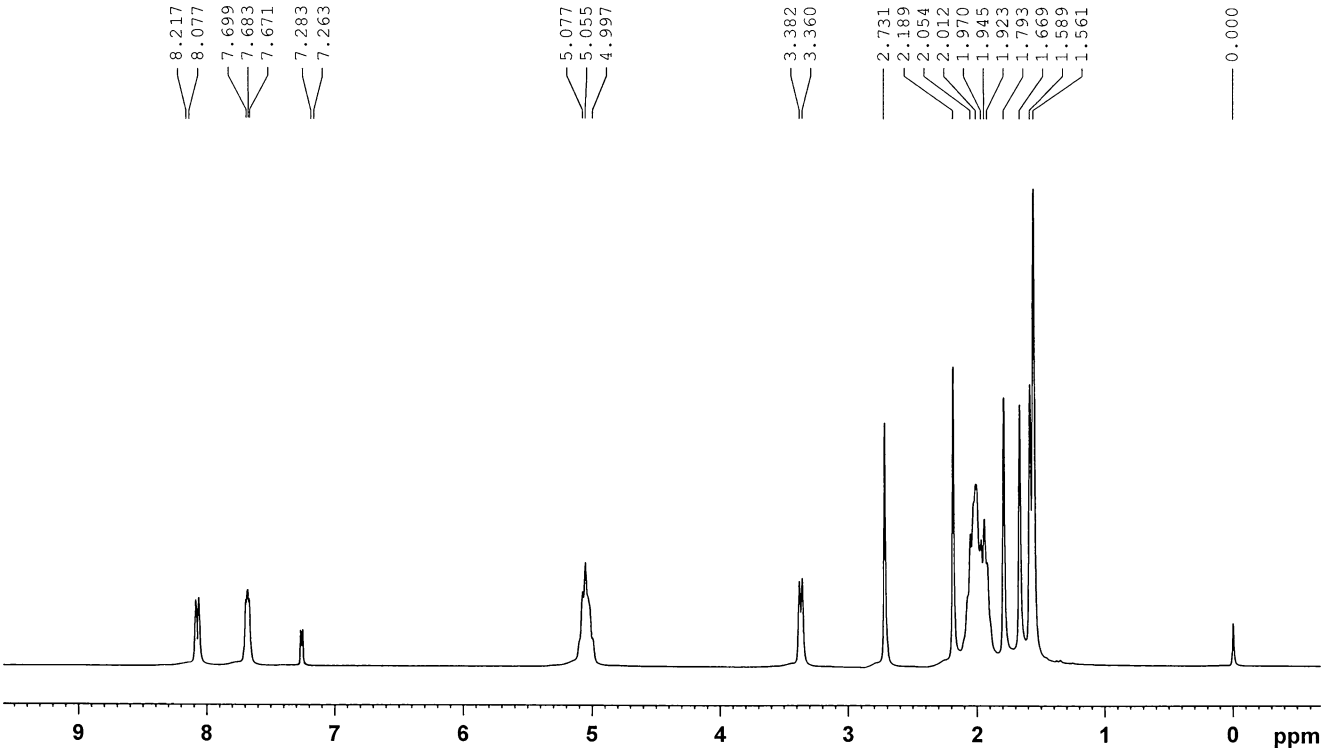

Fig. 3 ^{1}H NMR Spectra of the purified quinone dissolved in $CDCl_3$ using tetramethylsilane as an internal standard

electron transport of mammals utilizes a ubiquinone for maximal performance. Thus, in the present study, we have tried to elucidate the structure of the napthoquinone involved in TPMET of *E. histolytica* which may serve as a future chemotherapeutic target.

To explore the structural information of the quinone involved in TPMET we have isolated the quinone from the plasma membrane of *E. histolytica* trophozoites and purified it using reverse phase HPLC techniques and these purified quinones were then analysed by a wide array of

Table 1 Chemical shifts (δ) and splitting patterns for H^1 NMR spectra of the purified compound

	Chemical Shifts and Splitting Pattern
Aromatic Hydrogen	7.263 (aromatic proton at C6) (d)
	7.683 (aromatic proton at C7) (t)
	8.077 (peri proton at C5 and/or C8) (d)
Quinonoid Hydrogen (C-2)	–
Olefinic Hydrogen adjacent to Carbonyl	–
Olefinic Hydrogens present in C-3 multiprenyl side chain	4.997–5.077 (m)
Allylic methylene adjacent to ring	3.360 (d)
SCH_3 ring	–
Benzenoid Methyl (C5 or C8)	2.731(s)
Quinonoid methyl (C2)	2.189 (s)
Allylic methylenes in C3 multiprenyl side chain	1.923–2.054 (m)
Trans methyl next to ring in the first isoprene unit	1.793
Cis end of chain methyl	1.669
Trans internal methyl groups	1.561–1.589
Aliphatic methylenes	–
Aliphatic Methyl Groups i.e. methyl groups on saturated Carbon atoms	–

Chemical Shifts (δ) and Splitting Patterns of the different nature of hydrogen atoms present in the purified compound using tetramethylsilane as an internal standard.

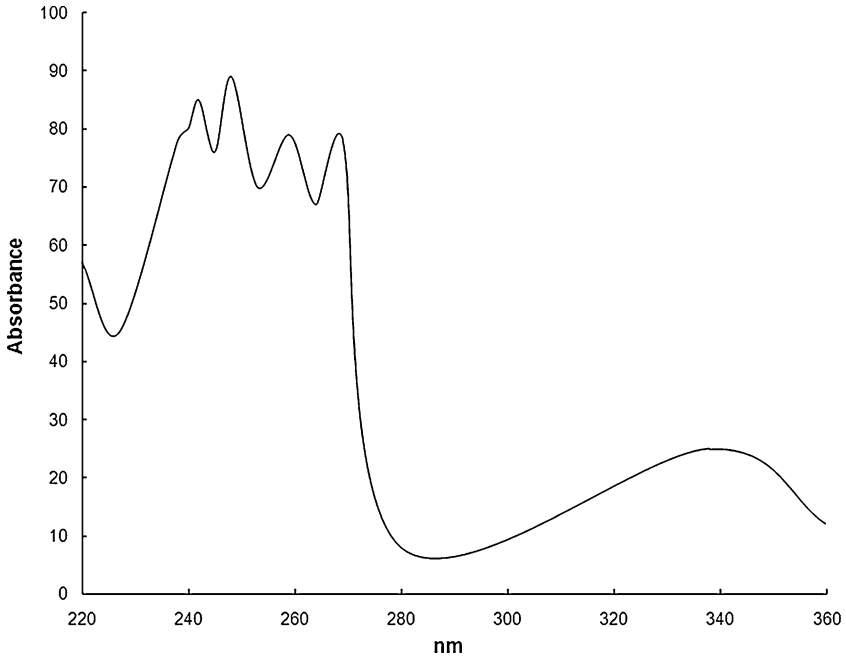

Fig. 4 Spectral fingerprint of the purified quinone as determined by wavelength scan between 220 and 360 nm. To analyse the spectral fingerprint of the HPLC purified quinone, it was evaporated to dryness and resuspended in isooctane

physicochemical techniques. Isoprenoid quinones are soluble in the usual lipid solvents; the most popular of these are acetone, diethyl ether, chloroform, ethanol, and petroleum ether (Dunphy and Brodie 1971). Adequate extraction of these components can be achieved with any one of these solvents or a mixture of two. Procedures which are extensively used are direct extraction of bacterial cells with acetone-petroleum ether (Booth 1959; Dunphy and Brodie 1971) or with a chloroforn-methanol (2:1, vol/vol) mixture (Collins et al. 1977; Dunphy and Brodie 1971). Both of these extraction procedures yield a complex mixture of lipids plus a small amount of nonlipid material. Isoprenoid quinones can be isolated from this mixture by a variety of chromatographic procedures. We have separated the isoprenoid quinones on reverse phase octadecylsilyl columns using polar mobile phase HPLC which is now extensively used to separate isoprenoid quinones. Reverse-phase chromatography facilitates the separation of isoprenoid quinone components according to their chain lengths and their degrees of unsaturation. The mobile phase composition can be varied in a gradient mode from more polar to less polar to achieve better separation. Identification can be done by comparing the retention time of known menaquinones. The isolated quinone gives a peak at a retention time close to

Table 2 Effect of different Ubiquinone and Napthoquinones on extracellular reduction of $K_3Fe(CN)_6$ and oxygen uptake by UV exposed *E. histolytica* trophozoites

Cell treatment	Rate of electron acceptor reduction, nmol/min/mg protein			
	Rate of $K_3Fe(CN)_6$ reduction	Relative Rate	Rate of Oxygen reduction	Relative Rate
UV unexposed EHC	1.14±0.21	100	8.16±0.91	100
UV unexposed EHC+HQNO	0.25±0.07	22	2.28±0.21	28
UV exposed EHC	0.51±0.09	45	2.20±0.17	27
UV exposed EHC+CoQ_{10}	0.55±0.05	48	2.61±0.15	32
UV exposed EHC+MQ-4	0.73±0.11	64	5.63±0.42	69
UV exposed EHC+TPQ-7	1.06±0.15	93	7.92±1.12	97

UV-unexposed and UV-exposed EHC (*E. histolytica* trophozoites) was prepared according to methods as given in experimental procedures. The viability of UV unexposed and exposed EHC was found to be ~95% for each experimental set. Quinones were added to EHC at a concentration of 30 μM, 10 min before the addition of electron acceptors. HQNO was added at a concentration of 10 μM where needed and pre-incubated with EHC for 10 min before the addition of electron acceptors. Ferricyanide reduction and Oxygen uptake was assayed according to the procedure as given in experimental procedures. Control experiments, which received equal volume of solvent (DMF) given along with the quinones, had no effect on either ferricyanide reduction or Oxygen uptake in EHC. The values represent the average of three experiments±S.D.

Menaquinone-4 (Fig. 1, Panel A & B). Thus, the purified quinone probably falls in the category of menaquinone as suggested from the Reverse Phase HPLC.

Purified isoprenoid quinones can be analyzed by using a variety of physicochemical techniques (Sommer and Kofler 1966). In particular, ultraviolet spectroscopy provides a simple method for investigating the category or class to which an unknown isoprenoid quinone belongs. Both menaquinones and phylloquinones (2,3-disubstituted quinones) exhibit qualitatively identical ultraviolet spectra, with five absorption maxima at 242, 248, 260, 269, and 326 nm and one point of inflection at 238 nm. Absorption bands at 242, 248, and 238 nm (shoulder) are due to benzenoid contributions, whereas bands at 260 and 269 nm are due to quinone absorption (Dunphy and Brodie 1971). However, removal of the methyl group from C-2 of the naphthoquinone nucleus (as in demethylmenaquinones and demethylphylloquinones) causes a shift in the quinone absorption contribution of about 6 nm to shorter wavelengths (λ_{max} 254 and 263 nm), whereas the benzenoid contributions (λ_{max}, 243 and 248 nm and 238 nm [point of inflection]) remain almost unaltered. Thus, ultraviolet spectrophotometry provides a simple method for distinguishing menaquinones and phylloquinones from their demethylated derivatives. Chlorobiumquinone (1′-oxomenaquinone-7) isolated from green photosynthetic bacteria (Frydman and Rapaport 1963; Redfearn and Powls 1968) exhibits ultraviolet absorption characteristics quite distinct from those of menaquinones and demethylmenaquinones, with λ_{max} at 254 nm in ethanol and a point of inflection at 265 nm (Powls et al. 1968). Thermoplasmaquinone, another methyl substituted naphthoquinone displayed absorption maxima at 242, 248, 259, 269 and 338 nm (Collins 1985a). This spectrum is similar to that of menaquinones, except that the band at 325 nm (in menaquinones) has shifted approximately 13 nm to higher wavelength. The two commonly encountered benzoquinones, plastoquinones and ubiquinones, also demonstrate characteristic spectral fingerprint. Plastoquinones show λ_{max} at 254 and 262 nm (isooctane), whereas in contrast, ubiquinones have a λ_{max} at about 270 to 275 nm and a second absorption band at 405 to 407 nm. The quinone purified from *E. histolytica* demonstrates absorption maxima at 242, 248, 259, 269 and 338 nm (Fig. 4) and hence the spectral fingerprint resembles with thermoplasmaquinone-7, which is a methylated derivative of menaquinone-7 (Collins 1985a).

The most precise and sensitive method for determining isoprenoid quinone structure is mass spectrometry. This method provides both accurate molecular weights of the isoprenoid quinones and structural information, such as the nature of the ring system, the length and degree of saturation of the isoprenyl side chain. When subjected to mass spectrometry, both menaquinones and ubiquinones produce characteristic fagmentation patterns. The base peaks in the mass spectra of menaquinones (including phylloquinone) occur at m/z 225 and are derived from the naphthoquinone nucleus. The mass spectrum of thermoplasmaquinone-7, a methylmenaquinone-7 had a base peak at *m/z* 239 with a second intense peak at *m/z* 201 (Collins 1985b). Ubiquinones and plastoquinones have corresponding nuclear fragments at m/z 235 and 189, respectively (Dunphy and Brodie 1971; Sommer and Kofler 1966). The mass spectrum of the purified quinone from the membrane of *E. histolytica* demonstrated a base peak at *m/z* 239 with a second intense peak at *m/z* 201 (Fig. 2, Panel A & B). Therefore, probably the purified quinone is a thermoplasmaquinone-7. The most intense peak for the purified quinone in the high mass region occurred at *m/z* 662, and was attributable to molecular ions (M^+) (Fig. 2, Panel A & B). This ion peak was larger than the corresponding ion peak of menaquinone-7 by 14-mass units, suggesting that this purified quinone compound has either a methyl group on the napthoquinone nucleus or ketonic oxygen at the side chain of menaquinone-7. The pattern of fragmentation of the isoprenoid substituent at the C-3 position of menaquinones is characteristic of the cracking pattern exhibited by polyisoprenoid chains in general. Fragmentation of the side chain under electron impact involves solely diallylic bonds. In the mass spectrum of thermoplasmaquinone-7 from *T. acidophilum* fragmentation of the side chain involves the loss of a terminal isoprenyl unit $(M-69)^+$, followed by five successive loss of 68 mass units (Collins 1985b). A peak of lower intensity was also observed at $(M-15)^+$ indicating a loss of a methyl group from the molecular ion. Saturation of an olefinic bond within the side chain of a menaquinone causes a marked alteration in the cracking pattern and provides information on the position of hydrogenation (Batrakov and Bergelson 1978). The mass spectrum of the purified quinone from *E. histolytica* membrane demonstrated a peak of lower intensity at 647 corresponded to the loss of CH_3 from M^+, whereas peaks of low intensity at *m/z* 593, 525, 457, 389, 321 and 253 were due to the sequential loss of 1 terminal (69 mass units) and 5 internal (68 mass units) isoprene units respectively. As 5 internal isoprene units of 68 mass units each has been lost during fragmentation, it can be assumed that the isoprenyl chain at C-3 contains 7 isoprenoid units. There is also no marked alteration in the cracking pattern indicating absence of saturation in the isoprenoid chain. Moreover, a peak at m/z 647 was also observed which is 15 mass units lower compared to M^+ and hence representing presence of an additional methyl moiety in the menaquinone-7. Furthermore, the presence of intense peaks at *m/z* 239 and 201 (derived from the naphthoquinone

nucleus) indicate that the additional methyl group is in the ring system and not in the polyprenyl side-chain. These fragmentation patterns and molecular ions are characteristic feature for methylmenaquinone-7. An isomeric compound oxomenaquinone-7 does not exhibit similar fragmentation pattern (Biswas et al. 2008). Thus the mass spectral data clearly indicates involvement of a thermoplasmaquinone-7, i.e. a methylmenaquinone-7 in TPMET of *E. histolytica*.

Proton NMR is also a powerful tool in the structural determination of the isoprenoid quinones. This technique yields in depth information about the chemical environment of the H atoms, the number of hydrogen atoms in each kind of environment, and the structure of groups adjacent to each hydrogen atom. The spectrum is normally recorded in deuterated chloroform or carbon tetrachloride with tetramethylsilane as an internal standard. Menaquinones and related 2,3-disubstituted naphthoquinones exhibit characteristic complex absorption at δ 7.5 to 8.1 due to the presence of four adjacent ring protons (Collins 1985b). In the NMR spectra of the purified quinone of *E. histolytica* an almost similar pattern of complex absorption was observed in the δ 7.2–8.1 region (Fig. 3, Table 1), due to the presence of 3 aromatic protons. The splitting pattern of the same indicated the presence of a methyl group in a peri-position on the ring system (C-5 or C-8). Demethylmenaquinones produce almost similar spectra to menaquinones except that a signal occurs at δ 6.7 due to quinonoid hydrogen while the singlet δ 2.1 to 2.2 is due to the C-2 methyl being absent (Collins 1985b). In the spectra of the purified quinone no signal is obtained for quinonoid hydrogen at the C-2 position characteristic of demethylmenaquinones (Fig. 3, Table 1). A signal is also not obtained for aliphatic hydrogen adjacent to carbonyl (Fig. 3, Table 1). This indicates the purified quinone is not either a demethylmenaquinone or an oxomenaquinone-7. Broad absorption at δ 5.0 to 5.2 is attributable to olefinic protons whereas the presence of a doublet at δ 3.3 to 3.4 is due to a methylene group adjacent to the ring (the latter is characteristic of all isoprenoid quinones containing a double bond in the first C5 unit) (Collins 1985b). Similar signals can be found in the NMR spectra of the purified quinone at δ 4.9–5.1 for the olefinic protons of C-3 multiprenyl side-chain and at δ 3.36 for allylic methylene just adjacent to the ring (Fig. 3, Table 1). The methyl substituents at the C-2 position of menaquinone and phylloquinone produce a singlet at δ 2.1 to 2.2 (Collins 1985b). In the NMR spectra of the purified compound a similar singlet at δ 2.18 was also found for the C-2 ring methyl group (Fig. 3, Table 1). Menaquinones also display strong bands in the δ 1.5 to 2.0 region due to methylene and methyl groups adjacent to double bonds. The methylenes appear around δ 1.9 to 2.0 and the olefinic methyls from δ 1.5 to 1.8 (Collins 1985b). Similar signals are also obtained at δ 1.92–2.05 for -CH_2-allylic; δ 1.79 for trans-CH_3 next to ring; δ 1.67 for cis-CH_3 end of chain; and δ 1.56–1.59, trans internal CH_3 of the C-3 multiprenyl side chain of the purified quinone (Fig. 3, Table 1). In phylloquinone and partially saturated menaquinones these signals occur at δ 1.2 to 1.3 for methylene groups and δ 0.8 to 0.9 for protons of methyl groups on saturated Carbon atoms (Collins 1985b). The spectrum of methionaquinone is similar to that of hydrogenated menaquinones except for ring methyl resonance. A singlet is observed at δ 2.6 due to the presence of SCH_3 (ring) whereas the singlet at δ 2.1 to 2.2 is attributable to absence of C-2 methyl (Collins 1985b). Thus, the NMR spectrum gives a clear idea that the purified quinone is a methylmenaquinone and mass spectral data suggests the presence of 7 isoprenoid units in the C-3 multiprenyl side chain. Therefore, the purified quinone involved in TPMET is a methylmenaquinone-7, i.e. a thermoplasmaquinone-7.

The TPMET and subsequently the non permeable electron acceptor reduction are impaired in *E. histolytica* trophozoites by UV irradiation. It had been demonstrated that the UV irradiation destructs the quinone and the quinone is then unable to act as a mobile electron carrier (Table 2). Further investigation indicates that the purified thermoplasmaquinone-7 restores the TPMET activity completely, whereas the menaquinone-4 restores the same partially and CoQ_{10} was unable to restore it (Table 2). A similar restoration of the TPMET activity of *L. donovani* using purified oxomenaquinone-7 was demonstrated by Biswas et al. (2008). This also gives additional evidence that the quinone involved in TPMET of *E. histolytica* trophozoites is probably a thermoplasmaquinone-7.

The analysis of the quinone purified from the plasma membrane fraction of *E. histolytica* using different physicochemical techniques and analysis of the restoration of TPMET activity in UV irradiated trophozoites clearly revealed the involvement of thermoplasmaquinone-7, a napthoquinone in TPMET of *E. histolytica*. In contrary, Ellis et al. (1994) had demonstrated presence of a small quantity of CoQ_9 in *E. histolytica*. We have also found a small proportion of CoQ_9 along with thermoplasmaquinone-7 when we purified quinone from the whole cell lipid extract of *E. histolytica* (data not shown). However, thermoplasmaquinone-7 has only been observed when the plasma membrane fraction was analyzed. Therefore, the ubiquinone is not present in the plasma membrane of the parasite and is not involved in TPMET activity. This is further confirmed by the results of restoration of TPMET activity, where it has been observed that ubiquinones fail to restore the TPMET activity of UV irradiated trophozoites. Moreover, the subcellular location of CoQ_9 and its functional role in *E. histolytica* awaits elucidation. Presence of thermoplasmaquinone-7 in TPMET chain in *E. histolytica*

reveals a major difference between host and parasite TPMET chain and can be used as a novel target for future rational chemotherapeutic drug deigning.

The metabolism of *E. histolytica* seems to have been shaped by secondary gene loss and lateral gene transfer, primarily from bacterial lineages (Loftus et al. 2005). The thermoplasmaquinone-7 was also found to be present in a thermophlic, acidophilic archaebacterium *Thermoplasma acidophilum*. *E. histolytica* has probably acquired the genes responsible for menaquinone biosynthesis by lateral gene transfer from the archae. This provides a powerful evidence for their evolutionary relationship with the archae and strongly confirms the point that it has branched out early during evolution and can be recognized as an early branching eukaryote.

Acknowledgement The authors are thankful to Indian Council of Medical Research for funding the study.

References

Aley SB, Scott WA, Cohn ZA (1980) Plasma membrane of *Entamoeba histolytica*. J Exp Med 152:391–404

Avron M, Shavit NA (1963) Sensitive and simple method for determination of ferrocyanide. Anal Biochem 6:549–554

Batrakov SG, Bergelson LD (1978) Lipids of the streptomycetes. Structural investigation and biological interrelation. Chem Phys Lipids 21:1–29

Bera T, Nandi N, Sudhahar D, Akbar MA, Sen A, Das P (2006) Preliminary evidence on existence of transplasma membrane electron transport in *Entamoeba histolytica* trophozoites: a key mechanism for maintaining optimal redox balance. J Bioenerg Biomembr 38:299–308

Biswas S, Haque R, Bhuyan NR, Bera T (2008) Participation of chlorobiumquinone in the transplasma membrane electron transport system of *Leishmania donovani* promastigote: effect of near-ultraviolet light on the redox reaction of plasma membrane. Biochim Biophys Acta 1780:116–127

Booth VH (1959) The extraction of pigments from plant material. Analyst (London) 84:464–465

Brodie AF (1963) Isolation and photoinactivation of quinone coenzymes. Meth Enzymol 6:295–308

Brodie AF, Ballantine J (1960) Oxidative phosphorylation in fractionated bacterial system II. The role of vitamin K. J Biol Chem 235:226–231

Bruchhaus I, Tannich E (1994) Induction of the iron-containing superxoide dismutase in *Entamoeba histolytica* by a superoxide anion-generating system or by iron chelation. Mol Biochem Parasitol 67:281–288

Bruchhaus I, Richter S, Tannich E (1998) Recombinant expression and biochemical characterization of an NADPH:flavin oxidoreductase from *Entamoeba histolytica*. Biochem J 330:1217–1221

Bruchhaus I, Richter S, Tannich E (1997) Removal of hydrogen peroxide by the 29 kDa protein of *Entamoeba histolytica*. Biochem J 326:785–789

Brzóska MM, Kamiński M, Supernak-Bobko D, Zwierz K, Moniuszko-Jakoniuk J (2003) Changes in the structure and function of the kidney of rats chronically exposed to cadmium. I. Biochemical and histopathological studies. Arch Toxicol 77:344–352

Bull H, Murray PG, Thomas D, Fraser AM, Nelson PN (2002) Acid phosphatases. Mol Pathol 55:65–72

Collins MD (1985a) Structure of thermoplasmaquinone from *Thermoplasma acidophilum*. FEMS Microbiol Lett 28:21–23

Collins MD (1985b) Analysis of isoprenoid quinones. Method Microbiol 18:329–66

Collins MD, Fernandez F (1984) Menaquinone-6 and thermoplasmaquinone-6 in *Wolinella succinogenes*. FEMS Microbiol Lett 22:273–276

Collins MD, Jones D (1981) Distribution of isoprenoid quinone structural types in bacteria and their taxonomic implication. Microbiol Rev 45:316–354

Collins MD, Pirouz T, Goodfellow M, Minnikim DE (1977) Distribution of menaquinones in actinomycetes and corynebacteria. J Gen Microbiol 100:221–230

Crane FL, Navas P (1997) The diversity of coenzyme Q function. Mol Asp Med 18:s1–s6

Crane FL, Morre DJ, Löw H (eds) (1989) Plasma membrane oxidoreductase in control of animal and plant growth. Plenum, New York

Diamond LS, Harlow DR, Cunnick CC (1978) A new medium for the axenic cultivation of *Entamoeba histolytica* and other *Entamoeba*. Trans R Soc Trop Med Hyg 72:431–432

Dunphy PJ, Brodie AF (1971) The structure and function of quinones in respiratory metabolism. Meth Enzymol 18:407–461

Ellis JE, Setchell KDR, Kaneshiro ES (1994) Detection of ubiquinone in parasitic and free-living protozoa, including species devoid of mitochondria. Mol Biochem Parasitol 65:213–224

Evans DJ Jr (1969) Membrane adenosine triphosphatase of *Escherichia coli*: activation by calcium ions and inhibition by monovalent cations. J Bact 100:914–922

Fine J (1935) The biuret method of estimating albumin and globulin in serum and urine. Biochem J 29:799–803

Frydman B, Rapaport H (1963) Nonchlorophyllous pigments of *Chlorella thiosulfatophilum* in chlorobiumquinone. J Am Chem Soc 85:823–825

Ishii M, Kawasumi T, Igarashi Y, Kodama T, Minoda Y (1987) 2-Methylthio-1,4-naphthoquinone, a unique sulfur-containing quinone from a thermophilic hydrogen-oxidizing bacterium, *Hydrogenobacter thermophilus*. Agric Biol Chem 47:167–169

Itoh T, Funabashi H, Katyama-Fujimura Y, Iwasaki S, Kuraishi H (1985) Structure of methylmenaquinone-7 isolated from *Alteromonas putrefaciens* IAM12079. Biochim Biophys Acta 840:51–55

Larm J, Vaillant F, Linnanne AW, Lawen AJ (1994) Up-regulation of the plasma membrane oxidoreductase as a prerequisite for the viability of human Namalwa rho O cells. J Biol Chem 269:30097–30100

Leuisse E, Labbe P (1992) Iron reduction and transplasma membrane electron transfer in the yeast *Saccharomyces cerevisiae*. Plant Physiol 100:769–777

Loftus B, Anderson I, Davies R, Alsmark UC, Samuelson J, Amedeo P, Roncagha P, Berriman M, Hirt RP, Mann BJ, Nozaki T, Suh B, Pop M, Duchene M, Ackers J, Tannich E, Leippe M, Hofer M, Bruchhaus I, Willhoeft U, Bhattacharya A, Cillingworth T, Churcher C, Hance Z, Harris B, Harris D, Jagels K, Moule S, Mungall K, Ormond D, Squares R, Whitehead S, Quail MA, Rabbinowitsch E, Norbertczak H, Price C, Wang Z, Guillen N, Gilchrist C, Stroup SE, Bhattacharya S, Lohia A, Foster PG, Sicheritz-Ponten T, Weber C, Singh U, Mukherjee C, El-Sayed NM, Petri Jr. WA, Clark CG, Embley TM, Barrell B, Fraser CM, Hall N (2005) The genome of the protist parasite *Entamoeba histolytica*. Nature 433:865–868

Lowry OH, Rosebrough NJ, Farr AL, Randall RJ (1951) Protein measurement with Folin phenol reagent. J Biol Chem 193:265–275

McLaughlin J, Muller M (1979) Calcium dependent ATPase in *Entamoeba histolytica*. J Protozool 26:10 (Abstr.)

Peters TJ, Muller M, de Duve C (1972) Lysosomes of the arterial wall. I. Isolation and subcellular fractionation of cells from normal rabbit aorta. J Exp Med 136:1117

Powls R, Redfearn ER (1969) Quinones of the chlorobacteriaceae. Properties and possible function. Biochim Biophys Acta 172:429–437

Powls R, Redfearn ER, Trippett S (1968) The structure of chlorobiumquinone. Biochem Biophys Res Commun 33:408–411

Ramos-Martínez E, Olivos-García A, Saavedra E, Nequiz M, Sánchez EC, Tello E, El-Hafidi M, Saralegui A, Pineda E, Delgado J, Montfort I, Pérez-Tamayo R (2009) *Entamoeba histolytica*: oxygen resistance and virulence. Int J Parasitol 39:693–702

Ravdin JI (1988) Human infection by *Entamoeba histolytica*. In: Ravdin JI (ed) Amoebiasis: human infection. Wiley, New York, pp 166–76

Redfearn ER, Powls R (1968) The quinones of green photosynthetic bacteria. Biochem J 106:50P

Reeves RE, Montalvo FE, Lushbaugh TS (1971) Nicotinamide-adenine dinucleotide phosphate-dependent alcohol dehydrogenase. Enzyme from Entamoeba histolytica and some enzyme inhibitors. Int J Biochem 2:55–64

Roy S, Sen CK, Tritschler HJ, Packer L (1997) Modulation of cellular reducing equivalent homeostasis by α-lipoic acid: mechanism and implications for diabetes and ischemic injury. Biochem Pharmacol 53:393–399

Santi-Rocca J, Marie-Christine R, Guillén N (2009) Host-microbe interactions and defense mechanisms in the development of amoebic liver abscesses. Clin Microbiol Rev 22:65–75

Sommer P, Kofler M (1966) Physiochemical properties and methods of analysis of phylloquinones, menaquinones, ubiquinones, plastoquinones, menadione and related compounds. Vit Horm (NY) 24:349–399

Stocker R, Suarna C (1993) Extracellular reduction of ubiquinone-1 and-10 by human Hep G2and blood cells. Biochem Biophys Acta 1158:15–22

Strober W (2001) Trypan blue exclusion test of cell viability. Current Protocols in Immunol. Appendix 3, Appendix 3B.

Sun IL, Sun EE, Crane FL, Moore DJ, Lindgren A, Low H (1992) Requirement of coenzyme Q in plasma membrane electron transport. Proc Natl Acad Sci USA 89:11126–11130

Tausky HH, Shor E (1953) A micrometric method for the determination of inorganic phosphorus. J Biol Chem 202:675–685

Umbreit WW, Burris RH, Stauffer JW (1957) Manomeric techniques. Burgers Publishing Co, Minneapolis MN, pp 1–85

World Health Organization. The world health report 1998. Life in the 21st century: a vision for all. World Health Organization, Geneva